

Contents lists available at [ScienceDirect](https://www.sciencedirect.com)

Science of the Total Environment

journal homepage: www.elsevier.com/locate/scitotenv

Effects of forest thinning on sap flow dynamics and transpiration in a Japanese cedar forest

Shin'ichi Iida^{a,*}, Shoji Noguchi^b, Delphis F. Levia^{c,d,e}, Makoto Araki^a, Kyohei Nitta^f, Satoru Wada^f, Yoshito Narita^g, Hiroki Tamura^f, Toshio Abe^h, Tomonori Kaneko^{f,i}

^a Department of Disaster Prevention, Meteorology and Hydrology, Forestry and Forest Products Research Institute, 1 Matsunosato, Tsukuba, Ibaraki 305-8687, Japan

^b Japan International Research Center for Agricultural Sciences, 1-1 Ohwashi, Tsukuba, Ibaraki 305-8686, Japan

^c Department of Geography & Spatial Sciences, University of Delaware, Newark, DE 19716, USA

^d Department of Plant & Soil Sciences, University of Delaware, Newark, DE 19716, USA

^e Department of Civil & Environmental Engineering, University of Delaware, Newark, DE 19716, USA

^f Akita Forestry Research and Training Center, 47-2 Idojiridai Kawabetoshima, Akita, Akita 019-2611, Japan

^g Forestry Environment Preservation Division, Akita Prefectural Government, 4-1-1 Sannou, Akita, Akita 010-8570, Japan

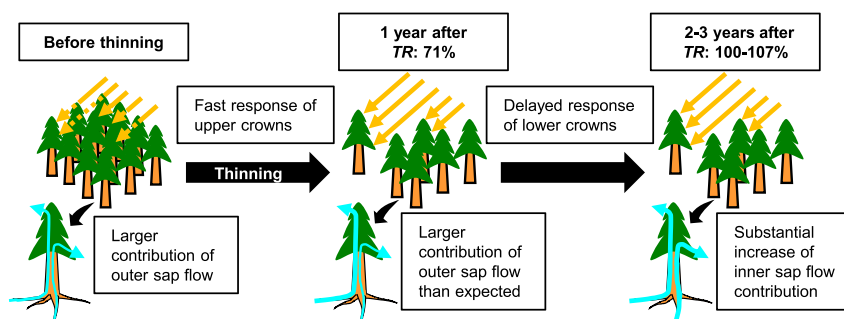
^h Tohoku Research Center, Forestry and Forest Products Research Institute, 92-25 Nabeyashiki, Shimokuriyagawa, Morioka, Iwate 020-0123, Japan

ⁱ Akita Prefecture Forestry Labor Countermeasures Fund, 8-28 Kawamotoyamashita, Akita, Akita 010-0931, Japan

HIGHLIGHTS

- Transpiration (TR) was measured for two years before and three years post thinning.
- Outer sap flux increased immediately, while inner increase was delayed.
- TR decreased to 71 % just after thinning, returning to initial levels in 2–3 years.
- Delayed but substantial increase of inner sap flow is a main factor for TR variation.
- Both outer and inner sap fluxes must be quantified to evaluate thinning effects.

GRAPHICAL ABSTRACT



ARTICLE INFO

Editor: Elena Paoletti

Keywords:

Thinning
Transpiration
Japanese cedar
Inner sap flux density
Outer sap flux density
Light conditions

ABSTRACT

Historically, forest thinning in Japan was conducted to obtain high-quality timber from plantations. Today, in contrast, thinning is also motivated by forest water balance and climate change considerations. It is in this context that the present study examines the effects of thinning on the ecophysiological responses of remaining trees, which are inadequately understood, especially in relation to changes in the magnitude and duration of transpiration. Sap flux densities were measured in both outer and inner sapwood to obtain stand-scale transpiration for two years in the pre-thinning state and three years post-thinning. The effects of thinning on transpiration were quantitatively evaluated based on canopy conductance models. The larger increases in outer sap flux density were found in the first year after the treatment, while those in inner sap flux density were detected in the second and third years. The remaining trees required a few of years to adjust to improved light conditions of the lower crown, resulting in a delayed response of inner sap flux density. As a result of this lag, transpiration was reduced to 71 % of the pre-thinning condition in the first year, but transpiration recovered to the pre-thinning

* Corresponding author.

E-mail address: iishin@ffpri.affrc.go.jp (S. Iida).

<https://doi.org/10.1016/j.scitotenv.2023.169060>

Received 14 September 2023; Received in revised form 29 November 2023; Accepted 30 November 2023

Available online 5 December 2023

0048-9697/© 2023 The Authors. Published by Elsevier B.V. This is an open access article under the CC BY-NC-ND license (<http://creativecommons.org/licenses/by-nc-nd/4.0/>).

levels in the second and third years due to compensating contributions from inner sap flow. In terms of more accurately chronicling the thinning effect, the distribution of sap flux density with respect to its radial pattern, is necessary. Such measurements are key to more comprehensively examining the ecophysiological response of forest plantations to thinning and, ultimately, its effect on the forest water balance.

1. Introduction

The bidirectionality of biosphere-atmosphere interactions, particularly under forest cover, has a substantial effect on the cycling of water and carbon as well as climate (Alkama and Cescatti, 2016; Ellison et al., 2017). Climate change can enhance or dampen some aspects of the coupled fluxes between forests and the atmosphere. For example, Amazonian deforestation has altered interactions between the land surface and atmosphere, causing decreases in rainfall (Leite-Filho et al., 2021; Smith et al., 2023; Spracklen and Garcia-Carreras, 2015). Plantation (or managed) forests may be even more vulnerable to the vagaries of climate change since they have a more uniform response likely partly stemming from a more homogenized hydrological cycle compared to natural forests (Levia et al., 2020). The interplay between managed forests and the atmosphere is especially relevant to Sustainable Development Goal (SDG) 6, which seeks to ensure access to water and sanitation for all (e.g., Creed and van Noordwijk, 2018). Japan, for example, thinned approximately 0.5 million ha of forest plantations in 2015 (Ohmasa et al., 2018). This is interfacial space where science can meet policy. How does forest thinning affect the ecophysiological and hydrological processes of managed forests? How does sap flux density and stand-scale transpiration (*TR*) change with thinning? Answers to such questions will require a quantitative estimate of the effect of thinning on hydrological cycle to provide the necessary information to help achieve SDG 6.

Evapotranspiration from a forest ecosystem affects the hydrological cycle and the processes of local precipitation recycling (Bonan, 2008; Ellison et al., 2017; Jones et al., 2020). For temperate forests, the ratio of runoff to precipitation was around 60 %, indicating that the evapotranspiration was equivalent to around 40 % of precipitation (Kosugi and Katsuyama, 2007; Shimizu et al., 2015). Thus, evapotranspiration is one of the most important processes of the hydrological cycle in forests. Forest evapotranspiration comprises three components—transpiration, interception loss and forest floor evaporation. Previous studies have reported the substantial contribution of transpiration to evapotranspiration, sometimes accounting for as much as 84.6 % for temperate forests (Wilson et al., 2001), 69.2 % for subhumid forest (Tie et al., 2018), and 73.7 % for tropical dry forest (Iida et al., 2020a). The quantitative estimation of transpiration is essential to understand the hydrological processes and climate system for forested areas.

Thinning is commonly applied to forest plantations with closed canopies to create suitable spaces among trees and to mitigate competition for light (especially for the lower crown), water and nutrients, thereby enhancing the growth of remaining trees and timber production (e.g., Lagergren et al., 2008; Skubel et al., 2017; Park et al., 2018). Most cases of thinning forests lead to reductions of transpiration because of the decrease in the sapwood area of a forest (e.g., Komatsu et al., 2013; Tateishi et al., 2015). However, it is necessary to investigate the effects of thinning on sap flux density of the remaining trees. For example, many cases of thinning have documented increases in sap flow amounts of the remaining trees (e.g., Morikawa et al., 1986; del Campo et al., 2022), which indicates the increase in sap flux densities of remaining trees is caused by exposure of crowns to improved light conditions (Medhurst et al., 2002). These changes in sap flux density correspond with the reports of increased growth rate of tree diameter in the post-thinning conditions (e.g., Mäkinen and Isomäki, 2004; Richardson et al., 2011). Thus, quantitative evaluations of changes for both stand sapwood area and stand-mean sap flux density are needed to more precisely comprehend the ecophysiological and hydrological responses

of remaining trees and to clarify the effects of thinning on transpiration.

While thinning has originally been employed to help ensure high quality timber production, we must now employ hydrology-oriented silviculture (Molina and del Campo, 2012; Onda and Gomi, 2021; del Campo et al., 2022) to clarify the hydrological responses of forests in the post-thinning condition and to adapt and/or mitigate the influences by a changing climate. It is important for these purposes to evaluate not only the degree of the effect of thinning on transpiration just after thinning, but also its dynamics over relatively longer time periods. del Campo et al. (2022) carried out a global meta-analysis of thinning studies from the viewpoint of hydrological processes and showed that the duration of thinning effect on transpiration ranged from 3 to 8 years following treatment with relatively large variations among site environments, species, and climates. Focusing on the effect of thinning on transpiration, previous studies have been disproportionately conducted in relatively dry areas as opposed to wet and humid areas (e.g., Tateishi et al., 2015; Wang et al., 2019), and, therefore, its intensive measurements are necessary, especially for stands in more humid areas that underwent thinning operations a few years prior.

Forests cover two-thirds of the land area of Japan, with Japanese cedar (*Crytomeria japonica* D. Don) and Japanese cypress (*Chamaecyparis obtusa* Sieb. et Zucc.) occupying roughly 20 % and 10 % of the forested area, respectively (Forestry Agency, Ministry of Agriculture, Forestry and Fisheries, Japan, 2022). Many plantations composed of these two species are unmanaged and consequently have high stand densities (e.g., Ohmasa et al., 2018). A similar situation has been reported in Spain (e.g., del Campo et al., 2019). Even though previous studies evaluated the effect of thinning on transpiration in both Japanese cedar and cypress stands (Morikawa et al., 1986; Komatsu et al., 2013; Sun et al., 2014; Tateishi et al., 2015), the magnitude and dynamics of the thinning effects over longer time spans remain unknown. To better understand how thinning affects transpiration, i.e., whether the effects on water resources is positive or negative, evaluation of the thinning-effect dynamics is necessary.

Here, we measured stand-scale transpiration based on the sap flow measurements in a thinned (by 38 % stand density) stand of Japanese cedar located in the northern part of Japan. It is hypothesized that thinning-induced improvement of solar radiation conditions could result in ecophysiological changes in the remaining trees by enhancement of sap movement, causing compensation of reduced transpiration by a decrease in stand-scale sapwood area. Our objectives are: (i) to evaluate the degree of decrease in transpiration by thinning and its temporal dynamics over a few of years after thinning; (ii) to clarify the effect of improved light conditions on transpiration, focusing on the difference between outer and inner sap flux densities; and (iii) to present a conceptual model to examine the changes in ecophysiological responses due to thinning. Achievement of these objectives would improve our understanding of the ecophysiological controls of thinning on water flux, thereby ultimately permitting a better integration among measurements, modeling, and policy as envisaged by Guswa et al. (2020).

2. Materials and methods

2.1. Study site

The target stand of Japanese cedar is located in a hilly area near Kaminosawa stream within the Nagasaka Experimental Watershed located in Akita Prefecture in northern Japan (40°16'N, 140°24'E, altitude: 84–174 m, Fig. S1). It was planted in 1963. In 2017, at 54 years of

age, the initial stand density was 1257 trees ha^{-1} (Table 1). Surficial geology is Neogene tuffaceous rock (green tuff) that has been weathered and softened (Kaneko et al., 2010). Annual mean precipitation and air temperature were 1905.7 mm and 10.3 °C, respectively, and the period without snow cover was generally from May to October (Noguchi et al., 2010).

Since the improvement cutting carried out in 1989, no silvicultural treatments have been applied to this stand. The first thinning was conducted from February to March 2017, during which 38 % stems, corresponding to 44 % of stand volume, were removed. Detailed information of thinning and stand characteristics including diameter at breast height (DBH) and tree height are listed in Table 1. Stand-scale transpiration (TR) based on the sap flow technique was measured for two years (2015 and 2016) and three years (2017, 2018 and 2019) in the pre- and post- and thinning conditions, respectively.

2.2. Measurements of micrometeorological conditions, leaf area index and canopy openness

Micrometeorological conditions were measured at the station in an open space toward the east-north-east 200-m from the Japanese cedar stand (Fig. S1). Measured factors are vapor pressure deficit (VPD) calculated from air temperature (T_a) and humidity (type HMP45A; Vaisala, Helsinki, Finland), solar radiation (S_d , type CNR4, Kipp & Zonen, Delft, The Netherlands) and gross rainfall (P , type B-071, Yokogawa Denshikiki, Tokyo, Japan). These factors were scanned every 30 s and recorded by a datalogger (type CR1000, Campbell Scientific, Logan, UT, USA) as the averaged or accumulated values over 10 min intervals. For the following analysis, we used daily amount of gross rainfall and daytime (9:00 to 15:00) mean values of air temperature, vapor pressure deficit and solar radiation. Measurements of micrometeorological conditions began in late 2015. Hence, summer 2015 data were estimated as follows: vapor pressure deficit was calculated by a regression equation derived from the vapor pressure deficit above the forest floor (VPD_{floor}) measured by a temperature/humidity probe (type S-THC-M002, Onset Computer Corporation, Bourne, MA, USA; $VPD = 1.632 \cdot VPD_{\text{floor}} + 2.756$, $R^2 = 0.78$). We estimated solar radiation with a regression equation obtained from the daily mean values calculated from daily duration of sunshine at Takanosu station ($S_{d\text{-taka}}$; Noguchi et al., 2010), which is 7 km apart from the stand and belonged to the Automated Meteorological Data Acquisition System (AMeDAS) managed by the Japan Meteorological Agency ($S_d = 2.619 \cdot S_{d\text{-taka}} - 32.092$, $R^2 = 0.89$). The volumetric soil water content was measured at the depths of 10, 30, 40, 60, and 90 cm by the time-domain-reflectometry sensors (type CS-616, Campbell Scientific, Logan, UT, USA). We calculated daily weighted mean value of soil water content to the depth of 90 cm (SWC) and used for the following analysis.

The leaf area index (LAI, $\text{m}^2 \text{m}^{-2}$) was measured at 22 points fixed in the stand with the Plant Canopy Analyzer (type LAI-2000, Li-Cor, Lincoln, NE, USA). At the same positions, we took hemispherical

Table 1

Stand characteristics of the measurement plot before and after thinning. Values in parentheses are ± 1 standard deviation.

	Before thinning	After thinning
Number of trees	16	10
Mean DBH (cm)	27.1 (6.2)	26.1 (3.8)
Mean height (m)	20.6 (1.9)	20.5 (1.4)
Mean height of lowest living branch (m)	11.5 (1.7)	11.6 (1.6)
Mean crown length (m)	9.2 (1.6)	8.9 (1.2)
Stand density (trees ha^{-1})	1257	786
Basal area ($\text{m}^2 \text{ha}^{-1}$)	76.1	43.1
Stand volume ($\text{m}^3 \text{ha}^{-1}$)	769.4	429.9
Mean sapwood width ^a (cm)	3.4 (0.5)	3.5 (0.4)

^a Sapwood width was measured in June 2015, and the other metrics in April 2016.

photographs (camera: D5100, Nikon, Tokyo Japan; lens: 4.5 mm F2.8 EX DC Circular Fisheye HSM, SIGMA, Kanagawa, Japan) and calculated the canopy openness for 0–10° zenith angle with HemiView (version 2.1, Delta-T Devices, Cambridge, UK).

The wood core samples were taken at the east and west sides of all stems within the plot by an increment borer to determine sapwood width in 2015 (Iida et al., 2017). The average of east and west sides was used as the sapwood width of each tree (Table 1). Note that Japanese cedar trees have a white zone near the boundary between sapwood and heartwood (e.g., Kumagai et al., 2007), in which the sap movement is inactive, and we excluded it from the sapwood width.

2.3. Estimation of stand-scale transpiration

The thermal dissipation method (TDM; Granier, 1985) was applied to measure sap flux density (F_d , $\text{cm}^3 \text{cm}^{-2} \text{h}^{-1}$) of all Japanese cedar trees within the plot ($n = 16$ in the pre-thinning condition, and $n = 10$ in the post-thinning condition) (Table 1, S1). A pair of 2-cm long probes were inserted into a stem, which were apart 15 cm vertically. The upper probe included a 0.2 W heater generating heat continuously, and the thermocouples of both probes measured the temperature difference between them (ΔT , °C). F_d can be calculated by the empirical equation (Granier, 1985) as:

$$F_d = 42.84 \cdot \left(\frac{\Delta T_0 - \Delta T}{\Delta T} \right)^{1.231} \quad (1)$$

where ΔT_0 is ΔT when F_d equals to zero, and we assumed the daily maximum of ΔT is the same as ΔT_0 (Iida et al., 2003). In this study, custom-made sensors were used (e.g., Kumagai et al., 2007), and ΔT was scanned every minute and 30-min averages were recorded by a datalogger with a multiplexer (type CR1000 and AM16/32B, Campbell Scientific, Logan, UT, USA).

Given the fact that underestimations of F_d have been reported (e.g., Steppe et al., 2010; Fuchs et al., 2017), we calibrated the TDM by using an equipment generating the artificial sap flow in cut segments by a vacuum pump (Shinohara et al., 2022; Iida et al., 2022). As a result, F_d obtained by Eq. (1) was found within ± 30 % of the artificial sap flux densities and did not indicate clear underestimations (Iida et al., 2020b), so that we applied Eq. (1) to calculate F_d .

It has been reported that F_d shows azimuthal and radial distributions in sapwood area (e.g., Shinohara et al., 2013). To consider the effect of azimuthal variations, we measured outer sap flux density at the depth from 0 to 2 cm (F_{d0-2}) in the sapwood at north and south sides of a tree, and obtained their averaged value (F_{d0-2}^-). Considering that all trees had the sapwood width of > 2 cm (i.e., sensor length), we measured inner sap flux density by an inner sensor installed at the depth from 2 to 4 cm (F_{d2-}) for trees whose sapwood width of ≥ 3 cm (Table S1). In cases where the inner sensors exceeded the active part of sapwood area, we applied the correction proposed by Clearwater et al. (1999). In the pre-thinning condition, a total of 46 sensors were used in 16 trees, with 29 sensors used in 10 trees in the post-thinning condition (Table S1). Based on the measurements, single-tree transpiration (Q , $\text{cm}^3 \text{h}^{-1}$) that accounted for contributions of outer and inner portions of sap flow was calculated as:

$$Q = Q_{0-2} + Q_{2-} = A_{S0-2} \cdot F_{d0-2}^- + A_{S2-} \cdot F_{d2-} \quad (2)$$

where Q_{0-2} and A_{S0-2} are sap flow ($\text{cm}^3 \text{h}^{-1}$) and sapwood area (cm^2), respectively, for the outer part in the depth from 0 to 2 cm, and Q_{2-} and A_{S2-} are for the inner part in the depth of > 2 cm, respectively (Table S2). Note that the total sapwood area of a tree (A_S) is the sum of the areas of outer and inner sapwood ($A_S = A_{S0-2} + A_{S2-}$).

The stand-scale transpiration (TR) can be calculated from the sum of Q for whole trees in the plot (ΣQ) as:

$$TR = \frac{\Sigma Q}{A_p} = TR_{0-2} + TR_{2-} = \frac{\Sigma Q_{0-2}}{A_p} + \frac{\Sigma Q_{2-}}{A_p} \quad (3)$$

where A_p is the plot area (127 m²), and TR_{0-2} and TR_{2-} are stand transpiration through the outer and inner parts of sapwood, respectively. TR , TR_{0-2} and TR_{2-} were obtained from the sap flow data of 16 and 10 trees for the pre- and post-thinning conditions, respectively (Table 1, S1). Moreover, we calculated the stand-scale transpiration of remaining trees (TR_{rem}) and their outer and inner sap flow contributions to TR_{rem} (TR_{rem0-2} and TR_{rem2-} , respectively) by excluding six thinned trees from the pre-thinning data. Then, the stand-scale mean sap flux density (J), and J through the outer (J_{0-2}) and inner sapwood (J_{2-}) were calculated as:

$$J = \frac{\sum Q}{\sum A_S} \quad (4)$$

$$J_{0-2} = \frac{\sum Q_{0-2}}{\sum A_{S0-2}} \quad (5)$$

$$J_{2-} = \frac{\sum Q_{2-}}{\sum A_{S2-}} \quad (6)$$

Iida et al. (2018) found that a serious underestimation of sap flux density occurred after a few of months from the insertion of sensors for Japanese cedar trees due to dehydration around the inserted sensor, and proposed a method to identify the dampening based on the relationship between vapor pressure deficit and sap flux density. Thus, all sensors were replaced with new ones every year, with a total of 179 sensors utilized over the five-year period (Table S1). We removed dampened sap flow data by this method, and replaced them with estimated values derived from the linear regression with sap flux density for the same tree. Table S3 shows the number of days available for analysis along with the corresponding gap ratios.

2.4. Calculation of canopy conductance and modeling of its environmental response

The canopy conductance (G) derived from the sap flow through the whole stand sapwood area was calculated with the simplified form of the Penman-Monteith equation (Monteith and Unsworth, 1990) as:

$$G = \frac{\gamma \cdot \lambda \cdot TR}{\rho \cdot C_p \cdot VPD} \quad (7)$$

where γ is the psychrometric constant, λ is the latent heat of vaporization of water, ρ is the density of moist air, C_p is the specific heat of air at constant pressure. The canopy conductance contributed by the outer (G_{0-2}) and inner (G_{2-}) parts of sap flow were obtained by substituting transpiration corresponding to the outer (TR_{0-2}) and inner parts of the sapwood (TR_{2-}) into Eq. (7), respectively. In the same manner, the conductance of the remaining trees in the pre-thinning condition (G_{rem}) and that contributed by outer (G_{rem0-2}) and inner (G_{rem2-}) sap flow were calculated by substituting TR_{rem} , TR_{rem0-2} and TR_{rem2-} into Eq. (7), respectively. Note that we obtained the daily average conductance using daytime mean vapor pressure deficit, thermodynamic variables based on daytime mean air temperature, and all version transpiration summed over 24 h, but divided by daytime values only (Phillips and Oren, 1998; Kumagai et al., 2008).

The environmental responses of the conductance can be expressed by a multiplicative-type function (e.g., Granier and Bréda, 1996; Kumagai et al., 2008). We took solar radiation, vapor pressure deficit and soil water content into account to evaluate the effect on conductance:

$$G = f(S_d) \cdot f(VPD) \cdot f(SWC) = \frac{S_d}{S_d + a} (b + m \cdot \ln VPD) (c + d \cdot \log_{10} SWC) \quad (8)$$

where a , b , c , d , and m are the fitting parameters, and b is the reference value of conductance at $VPD = 1$ kPa (Oren et al., 1999). For all types of conductance (G , G_{0-2} , G_{2-} , G_{rem} , G_{rem0-2} , G_{rem2-}), we derived the sets of parameters reflecting each environmental response. The fittings were

carried out for each year of pre-thinning condition (i.e., 2015 and 2016), whole pre-thinning dataset (i.e., two years of 2015 and 2016) and for each year of post-thinning period (i.e., 2017, 2018 and 2019).

In order to evaluate the effect of thinning on transpiration excluding the influences resulting from the year-to-year differences in environmental conditions (Fig. S2) and in measurement gaps over the five years (Table S3), we estimate all types of conductance (G , G_{0-2} , G_{2-} , G_{rem} , G_{rem0-2} , G_{rem2-}) based on the parameter sets (Table S4) with the same climatic input variables over the whole analysis period (i.e., 219 days from 2015 to 2019). Then, the calculations of stand-scale transpiration through whole sapwood (CT) were obtained from modeled conductance (G) and measured environmental variables over the 219 days of study (Eq. (7)). Similarly, transpiration contributed by outer and inner sap flow (CT_{0-2} and CT_{2-}) were calculated from the modeled values of outer and inner conductance (G_{0-2} and G_{2-}), respectively. In the same manner for the remaining trees in the pre-thinning condition, the stand-scale transpiration and the contributions by outer and inner sap flow (CT_{rem} , CT_{rem0-2} and CT_{rem2-}) were obtained from the modeled G_{rem} , G_{rem0-2} and G_{rem2-} , respectively. Finally, the effect of thinning on transpiration through the whole sapwood was detected as the difference in calculated transpiration values between the pre- and the post-thinning conductance models (ΔCT), and the same calculation procedure was applied for the outer and inner parts, ΔCT_{0-2} and ΔCT_{2-} , respectively. We also calculated the differences in whole sapwood transpiration for remaining trees (ΔCT_{rem}) as the subtraction of CT_{rem} from CT in the pre-thinning condition, and also for the outer and inner parts of the remaining trees (ΔCT_{rem0-2} and ΔCT_{rem2-} , respectively). Statistically significant differences in mean values of sapwood width were analyzed using paired t -test, while linear regression modeling was performed to all types of G values. All statistical analyses were conducted in R 4.3.1 (R Core Team, 2023).

3. Results

3.1. Forest conditions before and after the thinning

The number of Japanese cedar trees was reduced from 16 to 10 following thinning, equating to a removal of 38 % of tree stems (Table 1). The LAI of the stand was 3.4 m² m⁻² in the pre-thinning condition, and just after the thinning, it decreased to 0.8 m² m⁻² (Fig. 1A). LAI then gradually increased to 1.4 m² m⁻² in 2019, constituting 41 % of the pre-thinning condition. Assuming the Beer-Lambert law extinction coefficients for the cedar canopy are 0.52 and 0.61 (Gyokusen et al., 1994; Komatsu, 2020), LAI in 2017 and 2019 yielded solar radiation levels under the cedar canopy of 3.9–4.9 and 2.8–3.4 times larger than the pre-thinning condition, respectively.

On the other hand, the canopy openness changed from 33 % to 59 % by thinning, and gradually decreased to 52 % in 2019, corresponding to a 158 % of the pre-thinning level (Fig. 1B). These trends demonstrate that both LAI and canopy openness never reached pre-thinning levels over the three years after treatment.

Year-to-year changes in stand-scale sapwood area (A_S) are shown in Table 2. A_S declined from 3809.7 cm² to 2395.2 cm² with the decrease ratio of 37.1 % after the thinning. We measured the post-thinning sapwood widths in August 2018 and compared them with the same trees in pre-thinning condition. The difference in sapwood-width average between pre- and post-thinning was not significant (paired t -test, $p = 0.13$), which was consistent with the fact that DBH showed a near constant increase ratio of 0.5 cm year⁻¹ from 2015 to 2019 (Fig. 1C).

3.2. Sap flux densities before and after the thinning

To account for the response of sap flux density to solar radiation in the early morning, typical diurnal changes of stand-scale mean sap flux density for sunny conditions are presented in Fig. 2. Across the four

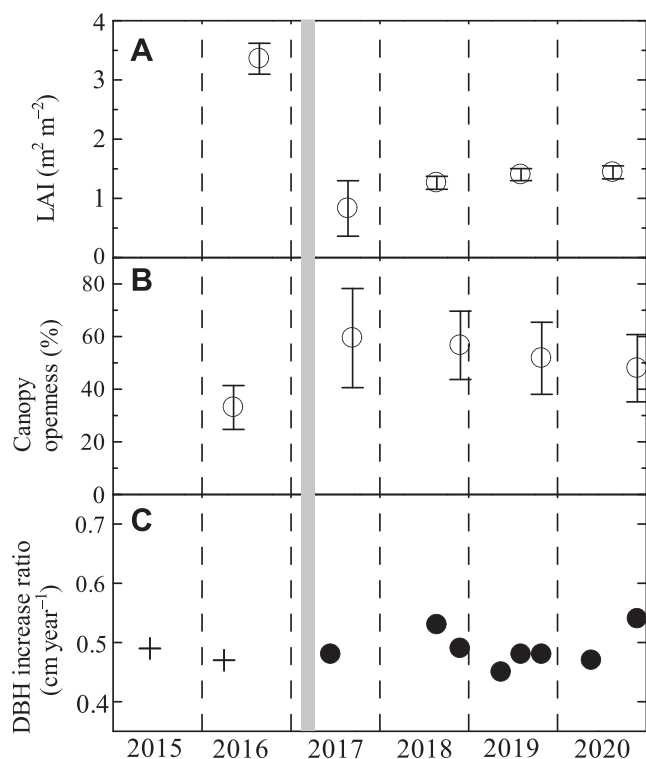


Fig. 1. Top (A) and middle (B) panels show time series of leaf area index (LAI) and canopy openness, respectively. Error bars depict the standard deviation. Bottom panel (C) indicates changes in the increase ratio of diameter at breast height (DBH) for four trees in the measurement plot. Crosses show the increase ratio from 2008 to 2015 ($0.49 \text{ cm year}^{-1}$) and 2008 to 2016 ($0.47 \text{ cm year}^{-1}$) corresponding to the pre-thinning condition, while black circles depict the ratios from 2016 to each measurement point. The gray colored band depicts the timing of the thinning treatment.

Table 2

Year-to-year variations of stand-scale sapwood area (A_s), along with its outer (A_{S0-2}) and inner (A_{S2-}) components.

Year	A_{S0-2} (cm^2)	A_{S2-} (cm^2)	A_s (cm^2)	Ratio to 2016 (%)	Decrease ratio (%)
Pre-thinning					
2015	2324.8	1409.9	3734.7	98.0	2.0
2016	2369.2	1440.5	3809.7	100.0	0.0
Post-thinning					
2017	1456.3	938.9	2395.2	62.9	37.1
2018	1503.1	972.7	2475.8	65.0	35.0
2019	1507.5	975.3	2482.8	65.2	34.8

years studied, a somewhat smaller solar radiation was measured in 2017, although large differences in its diurnal patterns were not detected across years (Fig. 2A). Sap flux density had the smallest value in the pre-thinning condition around noon in 2016, and increased gradually in the post-thinning period from 2017 to 2019 (Fig. 2C). Relatively large increases in outer sap flux density were detected in the first year after the thinning in 2017 and similar values were found in 2018, then slight increases in the morning were measured in 2019 (Fig. 2D). Although slight declines in inner sap flux density were observed just after the thinning, it showed larger and clear increases from 2017 to 2018 and 2018 to 2019 (Fig. 2E), indicating smaller effects of a slightly smaller vapor pressure deficit in 2018 (Fig. 2B). The response of inner sap flux density to sunrise is especially noteworthy as it got earlier and steeper. Interestingly, changes in inner sap flux density were more evident than those in whole and outer sap flux densities. For all data measured over

the five years regardless of solar radiation, the largest changes were measured in inner sap flux density (Fig. 2F, G, H) with similar relationships found for sunny diurnal patterns (Fig. 2C, D, E).

3.3. Stand-scale transpiration before and after the thinning

Stand-scale transpiration (TR) increased with vapor pressure deficit (Fig. 2I), and was similar between 2015 and 2016. Given that transpiration was measured in spring and early summer from 2016 to 2019, its maximum of 2.7 mm day^{-1} was found in the pre-thinning condition in 2016, whereas it decreased after thinning with a maximum of 1.9 mm day^{-1} . In the second and third years from thinning (2018 and 2019, respectively), increasing trends of transpiration were confirmed, resulting in an almost similar level as the pre-thinning condition (Fig. 2I).

3.4. Canopy conductance and its response to light, soil moisture and humidity

There were no clear relationships between canopy conductance (G) and solar radiation (Fig. 3A). The soil water content (SWC) was >0.33 except for 2019, in which it had the value close to 0.3, however, canopy conductance in 2019 showed the similar variations with the other years (Fig. 3C). On the other hand, the linear relationships between canopy conductance and vapor pressure deficit (VPD) in both of pre- and post-thinning conditions were found (Fig. 3B), and the fitting parameters of $f(\text{VPD})$, that is, b and m , were obtained for each year and two-year dataset from 2015 and 2016 (Eq. (8); Fig. 3B; Table S4). The values of $G/f(\text{VPD})$, which exclude effects of vapor pressure deficit on conductance, were distributed around unity over whole ranges in solar radiation and soil water content (Fig. 3D, E), strongly indicating that conductance was solely controlled by vapor pressure deficit. Note that similar trends were found for conductance, which reflects outer and inner sap flow contributions (G_{0-2} and G_{2-} , respectively; Figs. S3, S4). Also, conductance of the remaining trees in the pre-thinning condition (G_{rem}) showed a correlation with vapor pressure deficit (Fig. S5), and the contributions from outer ($G_{\text{rem}0-2}$) and inner ($G_{\text{rem}2-}$) sap flow exhibited similar relationships (Figs. S6, S7). Thus, all types of conductance were modeled by linear regressions with vapor pressure deficit (Table S4), which can reasonably calculate stand-scale transpiration (Fig. S8).

3.5. Quantification of the thinning effect based on the conductance model

The calculated transpiration by the conductance model for 2017 was 71 % of the pre-thinning condition, which was larger than that of the remaining trees in the pre-thinning condition (CT_{rem}) of 59 %, indicating a lesser effect on transpiration than expected from the pre-thinning response (Fig. 4A). The calculated transpiration by the models of 2018 and 2019 were 100 % and 107 %, respectively. Transpiration contributed by the outer sap flow (CT_{0-2}) were estimated to be 83 % in 2017, which was larger than that expected from the pre-thinning condition ($CT_{\text{rem}0-2}$) of 62 % (Fig. 4B). The contribution of outer sap flow in 2018 and 2019 resulted in 98 % and 97 % of the pre-thinning condition, respectively, and its increase slowed dramatically as pre-thinning levels were approached. On the other hand, the contribution of inner sap flow (CT_{2-}) of 49 % in 2017 was smaller than its expected value ($CT_{\text{rem}2-}$) of 54 % (Fig. 4C). Remarkable increases in inner sap flow contribution were found in 2018 and 2019 with values of 103 % and 125 %, respectively. Comparing these results among whole, outer and inner sap flow, the difference in calculated transpiration between the pre- and post-thinning condition (ΔCT) was mainly caused by the inner contribution (ΔCT_{2-}) rather than the outer (ΔCT_{0-2}) (Fig. 5B). Assuming outer and inner responses of the remaining trees as the same in the pre-thinning condition ($\Delta CT_{\text{rem}0-2}$ and $\Delta CT_{\text{rem}2-}$, respectively), the actual contribution of the outer part (ΔCT_{0-2}) was lower than $\Delta CT_{\text{rem}0-2}$, while that of inner effect (ΔCT_{2-}) was larger than $\Delta CT_{\text{rem}2-}$ in the first year after the thinning (Fig. 5A, B).

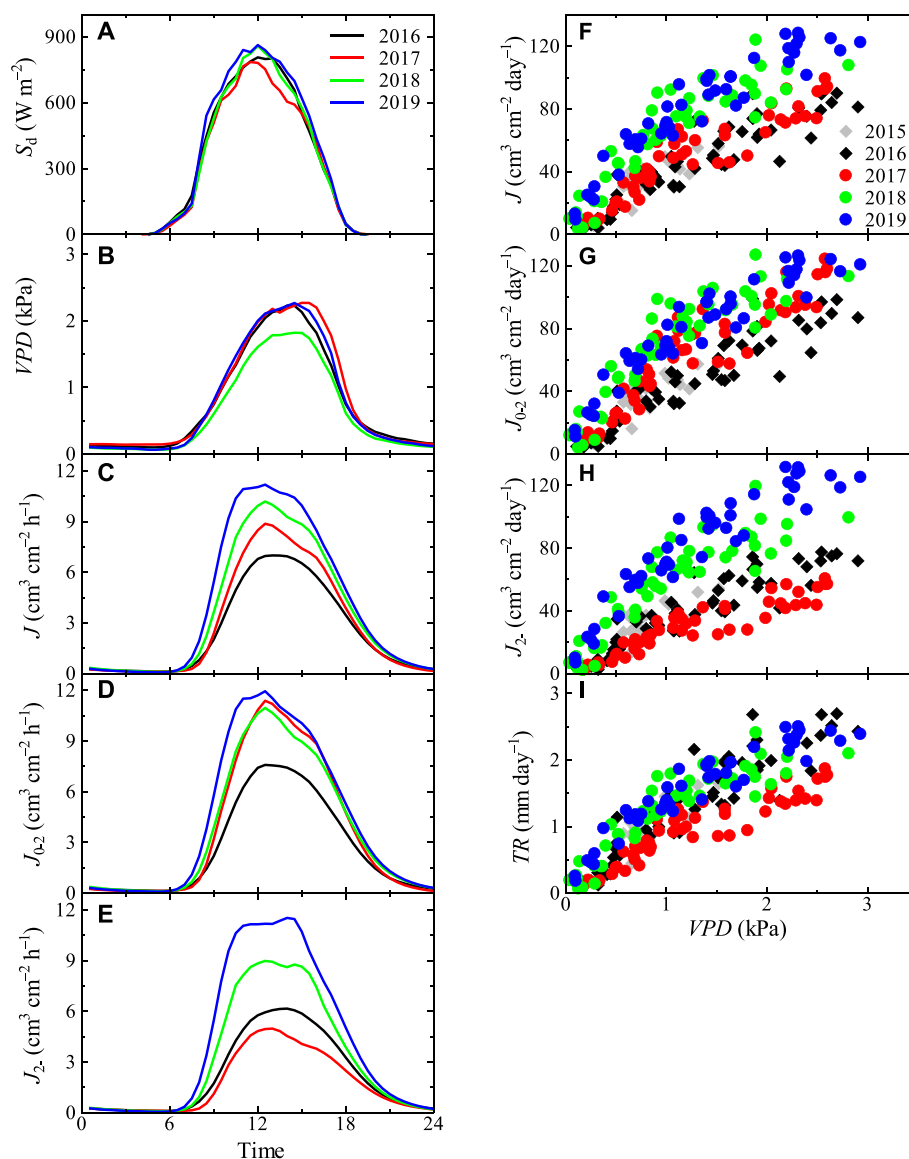


Fig. 2. Left panels indicate diurnal changes in (A) solar radiation (S_d), (B) vapor pressure deficit (VPD), (C) stand-scale sap flux density for whole sapwood area (J), (D) J in the outer sapwood area ($J_{0.2}$), and (E) J in the inner sapwood area (J_2). Data are selected for the days when the daytime mean S_d is >500 ($W m^{-2}$), encompassing 30, 19, 23 and 22 days for 2016, 2017, 2018 and 2019, respectively. Please note that to ensure comparability among the data collected we do not include data measured in 2015 due to seasonal differences in data collection. The 2015 data were acquired in summer when sunrise and sunset times were different, while for all the other years data were acquired in spring to early summer. Right upper three panels show comparisons between daytime mean vapor pressure deficit (VPD) and daily values of stand-scale sap flux density for (F) whole sapwood, (G) outer and (H) inner parts of sapwood. The right bottom panel (I) shows the relationship between VPD and daily stand-scale transpiration (TR).

4. Discussion

4.1. Changes in stand-scale transpiration before and after thinning

In 2017, the first year after thinning, stand-scale transpiration was 71 % of the pre-thinning level (Fig. 4A), and it was relatively larger than the remaining sapwood of 63 % (Table 2) and the value expected from the pre-thinning condition of 59 % (Fig. 4A). For Japanese cedar stands, when the sapwood area was reduced to 63 % of the pre-thinning condition, 56 % transpiration was estimated (Komatsu et al., 2013), and a value of 72 % transpiration was obtained for the case of 66 % sapwood (Tateishi et al., 2015). Thinning effects were also reported for Japanese cypress stands as 51 % transpiration for 55 % sapwood (Tateishi et al., 2015) and as 62 % transpiration for 54 % sapwood (Sun et al., 2014). Our result of 71 % transpiration for 63 % sapwood (Table 2) was comparable to these previous reports. Because transpiration is expressed as

the product of sapwood area and sap flux density (Eqs. (2)–(3)), the decreases in sapwood area contribute to reductions of transpiration in the first year after thinning.

Based on the comparisons between percentages of transpiration and sapwood area to the pre-thinning conditions, Komatsu et al. (2013) and Tateishi et al. (2015) concluded that the effects on sap flux density were relatively small and the decreases in transpiration were caused by the depletions in the sapwood area. However, in this study, the calculated transpiration in 2017 was larger than expected by assuming the same environmental responses of canopy conductance for the remaining trees as the pre-thinning condition (CT_{rem} , Fig. 4A). This means the increased sap flux density in the first year after the thinning, which was confirmed by the measurements (Fig. 2C, F), corresponding with the enhancement of single-tree transpiration of the remaining trees. The increase in sap flux density after thinning was found in Sun et al. (2014), and had been recognized as the general pattern based on the meta-analysis of thinning

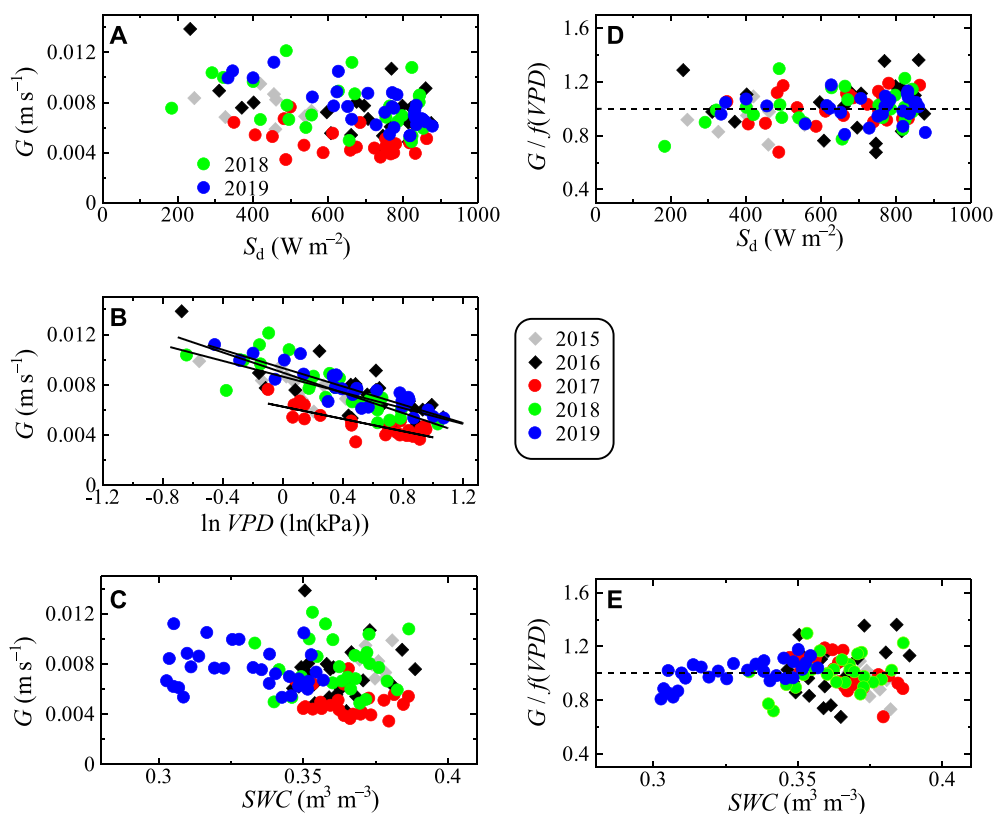


Fig. 3. The left panels show responses of canopy conductance (G) to daytime mean of (A) solar radiation (S_d) and (B) vapor pressure deficit (VPD), and (C) daily mean of soil water content (SWC). Solid lines depict the results of regression analysis (refer to Table S4). The right panels depict the relationships between G scaled by vapor pressure deficit function ($G/f(VPD)$) and (D) S_d , and (E) SWC . The dashed lines denote a $G/f(VPD)$ value of 1.

studies (del Campo et al., 2022). Thus, it is concluded that the first-year decrease in transpiration resulted from the decline in sapwood area, although this was partly compensated by the increased sap flux density.

The stand-scale transpiration recovered to pre-thinning level after more than two years (Fig. 4A), and the duration of effect by thinning was near the lower boundary of the range of the 3 to 8 year window reported by del Campo et al. (2022). Similarly, Bréda et al. (1995) found that the duration of the thinning effect on transpiration of a pure natural oak stand was two years post treatment. For a boreal forest consisting of Scots pine and Norway spruce in Sweden, 120 % stand-scale transpiration compared to the pre-thinning level was measured in the second year of the post-thinning condition (Lagergren et al., 2008). Considering these previous studies, our finding that the stand-scale transpiration increased to the pre-thinning condition after two years post treatment concurs with these other studies.

4.2. Changes in sap flux density by the thinning explained by ecophysiological factors

The increase in transpiration in the second and third years after thinning could not be attributed to changes in sapwood area, which showed negligible increases after the thinning (Table 2, Figs. 2I, 4). Therefore, the increase in sap flux density was the main factor explaining the recovery of transpiration (Fig. 2C, F). LAI and canopy openness, however, were 41 % and 158 % of pre-thinning levels in 2019, respectively (Fig. 1A, B). Given the fact that the foliage of the stand was less than in the pre-thinning condition, there is a clear indication that the ecophysiological response of remaining trees was altered due to the thinning. Specifically, the distribution of transpiration activity within the crowns of remaining trees could shift, resulting in larger changes in sap flux density originating from the inner than outer sapwood (Figs. 2D, E, G, H, 4B, C). In order to explain the difference between outer and

inner sap flow contributions due to the thinning, a conceptual model was created (Fig. 6).

Congruent with our findings, larger contributions of inner sap flux density after thinning were also found for other coniferous tree species and eucalypts (Medhurst et al., 2002; Fiora and Cescatti, 2006; Gebauer et al., 2011). Previous studies pointed out that the water flowing in the inner part of sapwood was supplied to the foliage on earlier-formed, or, lower branches (e.g., Dye et al., 1991; Forrester et al., 2012; Cermák et al., 2015; Fig. 6). Thus, the increase in inner sap flux density corresponds with thinning-induced improvement of light condition for remaining trees, especially for lower crowns. In the early morning with lower solar inclination angles, the degree of solar radiation reaching the lower part of tree crowns is more dependent on the lateral shadows cast by neighboring trees than upper portions of the tree crown. Therefore, it is expected that the most pronounced changes of inner sap flux density following thinning would occur in the early morning. Indeed, the responses of inner sap flux density around sunrise became earlier and sharper from the first to third year (Fig. 2E). These measurement results clearly indicate the importance of position vis-a-vis neighboring trees on inner/outer sap flux densities in relation to forest thinning (Fig. 6).

The different dynamics in sap flux density between the outer and inner parts of the sapwood was found after the thinning (Fig. 2D, E), and, thus, temporal variations should be considered as an important dimension of the ecophysiological responses of the cedar stand to thinning (Fig. 6). The rapid increase in the outer sap flow contribution to transpiration in the first year after thinning corresponded with Sun et al. (2014), followed by its relatively small changes in the second and third years after treatment (Figs. 2D, G, 4B). On the other hand, the inner contribution showed a decrease in the first year, and then increases for second and third years (Figs. 2E, H, 4C). These results are attributed to the differences in stomatal and photosynthetic response between sun-exposed and sun-shaded foliage in the crown (e.g., Pearcy and Sims,

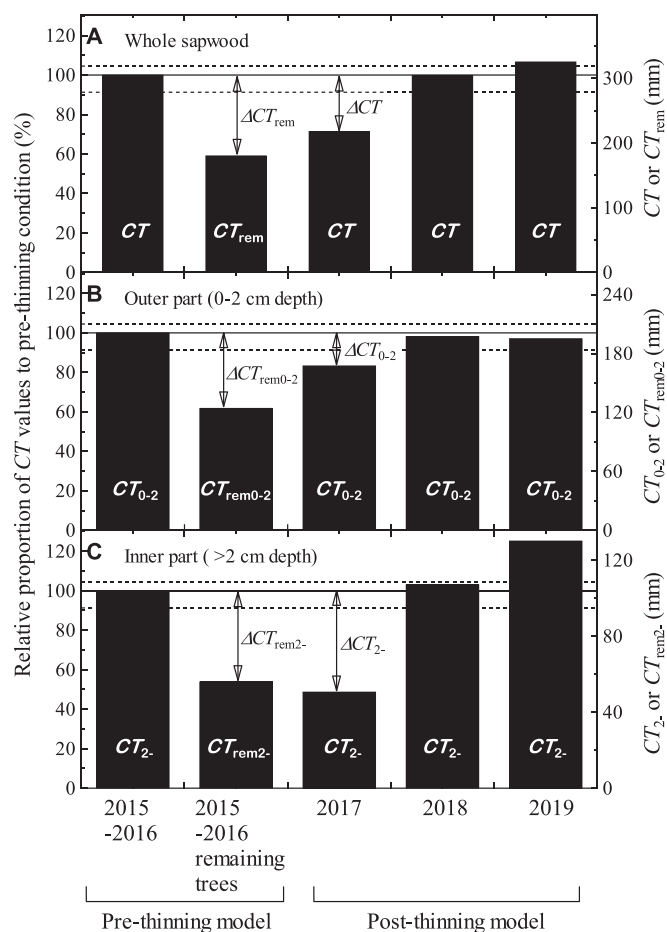


Fig. 4. Calculated amounts of stand-scale transpiration through (A) whole sapwood (CT), (B) outer (CT_{0-2}) and (C) inner (CT_{2-}) parts of sapwood based on the conductance models. The relative proportions of these values to pre-thinning condition are also shown. The solid lines indicate the results obtained from the model for the pooled dataset of the pre-thinning condition (2015–2016). The upper and lower dashed lines depict the amounts resulted from the models of 2016 and 2015, respectively. Refer to Table S4 for detailed information of each model. Arrows show differences in CT values between the pre-thinning condition and each period (ΔCT). Years 2017, 2018, and 2019 represent the first, second, and third years after thinning, respectively.

1994; Mohammed and Parker, 1999). The foliage in the upper part of crown, which originally had better light conditions, could have higher stomatal conductance than the lower crown, triggering higher sap flux density in outer than inner sapwood in the pre-thinning condition (Fig. 6). Moreover, sun-exposed foliage in upper crown could adapt more readily to the improved radiation environment, while the shade formed foliage in the lower crown would have a limited capacity to adjust the modified environment in the first year after the treatment (Harrington and Reukema, 1983; Mohammed and Parker, 1999; Fig. 6). In addition, the lower crowns of the remaining trees would be partly damaged during the thinning operations by the contacts of branches and/or boles of thinned trees (Fig. 6). These related to the lower crown were probably reasons to explain the slight decrease in inner sap flux density measured in the first year (Fig. 2E, H). The newly expanded foliage after the thinning would adjust to the improved light condition (Mohammed and Parker, 1999; Jiménez et al., 2008). Gebauer et al. (2014) pointed out that the remaining trees required a few of years to adjust the stomatal function of shade formed foliage to the thinning-induced changes in light condition, and similar responses could be detected in the second and third years (Fig. 6). Overall, different ecophysiological responses of the upper and lower crowns are

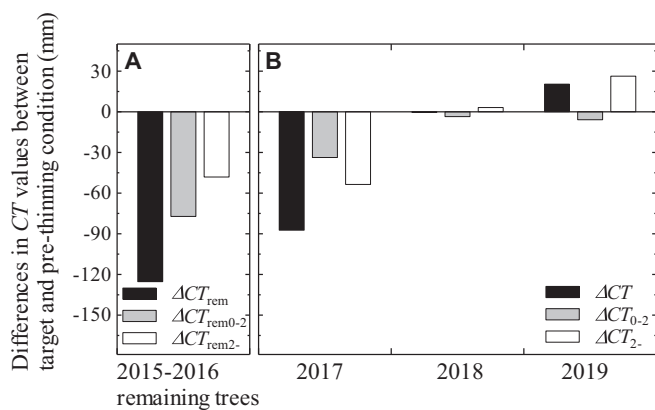


Fig. 5. The left panel (A) shows the differences between stand-scale transpiration calculated by the model including remaining trees only (CT_{rem}) and all trees in the pre-thinning condition for whole sapwood (ΔCT_{rem}), the outer (ΔCT_{rem0-2}) and inner sapwood (ΔCT_{rem2-}). The right panel (B) indicates differences between calculated stand-scale transpiration (CT) by each model of the post-thinning and the pre-thinning conditions for whole sapwood (ΔCT), the outer (ΔCT_{0-2}) and inner (ΔCT_{2-}) sapwood. Refer to Fig. 4 for the detailed definitions of ΔCT values. Years 2017, 2018, and 2019 represent the first, second, and third years after thinning, respectively.

summarized, and the processes causing these changes in transpiration after the thinning are shown as a conceptual model (Fig. 6).

4.3. Implications for future directions to investigate the effect of thinning

Our measurements clearly showed the ecophysiological changes of the remaining trees after thinning (Fig. 6). The increases in the inner contribution, which probably resulted from the improvement of light environment for the lower part of crown, caused the recovery of transpiration after the treatment. In terms of more accurately chronicling the thinning effect, both measurements of outer and inner sap flux densities are necessary. In cases that measurements are not carried out and/or the correction factors (Delzon et al., 2004) determined at the pre-thinning condition are used, the inner contribution is underestimated, and finally, the lower increases in transpiration would be obtained with a consequent misunderstanding of the longer effect by thinning. To measure the radial distribution of sap flux density with high spatial resolution over sapwood area, the heat field deformation method (Nadezhdina et al., 2012) is recommended. Our results also strongly suggest the necessity of taking account of outer and inner contributions into the calculation and/or prediction of changes in transpiration and its dynamics after thinning with the numerical simulations. It should be emphasized that longer measurements of sap flux density (i.e., > 5 years) at this site are difficult because TDM sensors need to be replaced yearly (Iida et al., 2018). Moreover, if sensors were replaced two or three times per year, the trees would have been damaged and reliable measurements of sap flow would have been compromised. Thus, to lengthen the measurement period in future studies, suitable sensor management schemes and/or other methods that are less damaging to the trees need to be developed.

The ecophysiological change after thinning, especially for the enhancement of the inner sap flow contribution to transpiration, would additionally suggest changes in the water transport process from the root system to the leaves. Specifically, water flowing in the inner part of sapwood would be absorbed from the deeper part of the root system (i.e., Cermák et al., 2015; Takeuchi et al., 2020). Measurement findings strongly suggest the larger water uptake by deep root system than shallow of Japanese cedar trees (Fig. 6). We observed the growth of understorey vegetation after the thinning because of increase in solar radiation to the subcanopy (Fig. S1D, E). Given the coexistence of overstorey cedar trees and understorey vegetation, the increase in the

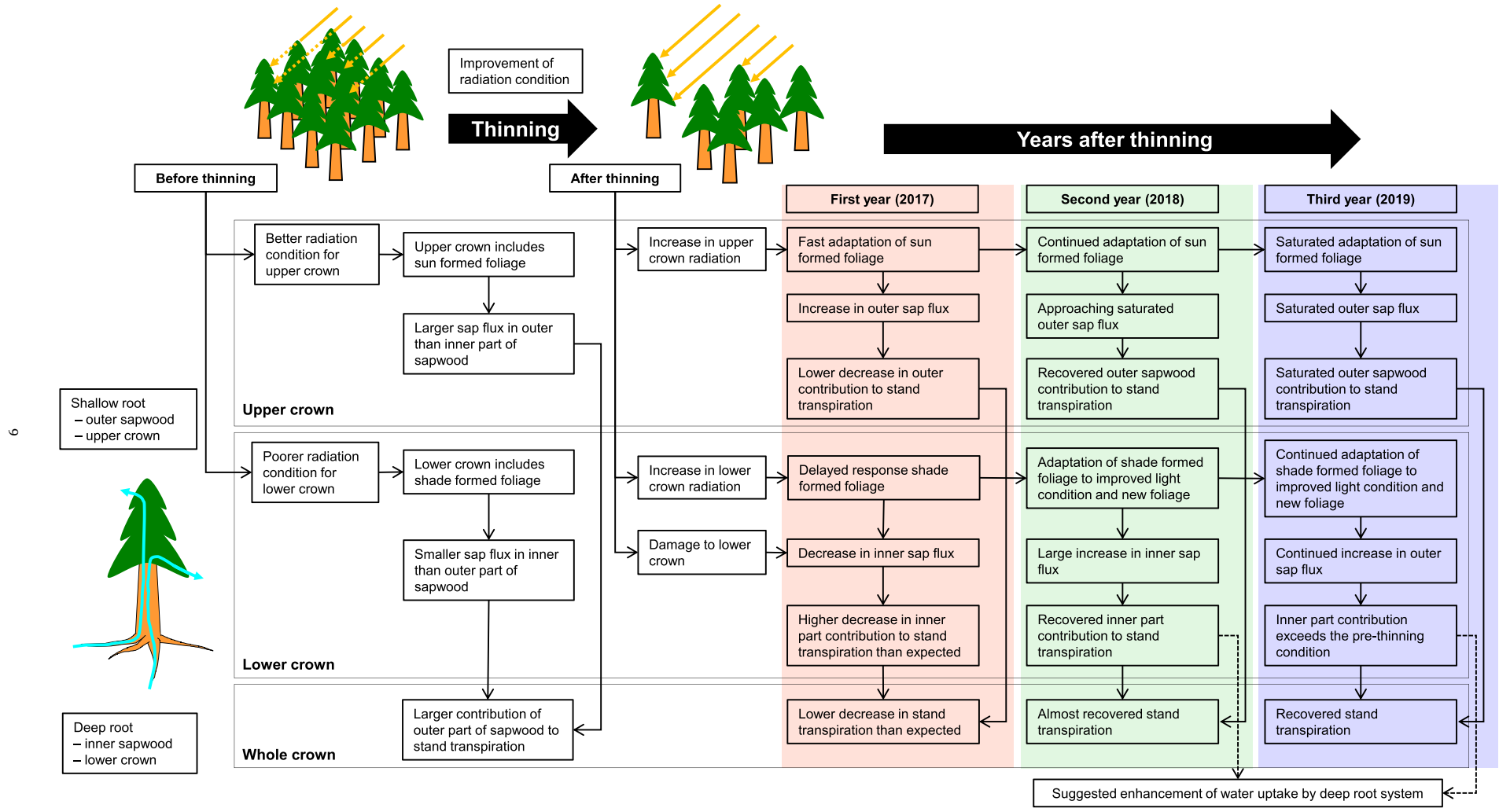


Fig. 6. A conceptual model showing the changes in stand-scale transpiration for the pre-thinning condition and three years following treatment. The conceptual model depicts the upper and lower canopy responses to the light improvement by the thinning.

inner contribution to cedar transpiration would be adaptive by water uptake through the relatively deeper roots, corresponding to the water source separation (e.g., Dawson et al., 2002; Yamanaka, 2018). The changes in water-uptake depth and/or water source separation might be essential for regulating the ecophysiological response of forest ecosystem after the thinning, and are recommended to be analyzed in future investigations for the comprehensive understanding the effect of thinning on forest water balance and the effect duration.

In addition to transpiration, the total water loss from a forest ecosystem includes interception loss and forest floor evaporation. The decreases in stand density caused the decrease in interception (Komatsu, 2007; Komatsu et al., 2008), and less LAI of overstory trees resulted in higher contribution of evapotranspiration from the understory vegetation to the whole evapotranspiration (Iida et al., 2020a). In fact, decreases in both transpiration and interception loss and an increase in forest floor evaporation were measured in the first year after the thinning (e.g., Sun et al., 2017). Recently, Chiu et al. (2022) found the contribution of regrown understory vegetation to evapotranspiration five months after thinning. The water loss from a Japanese cypress watershed recovered to the pre-thinning condition three years after thinning (Kubota et al., 2018), while the trend of transpiration after thinning was unknown. In order to understand the effect of thinning on the forest water balance and its dynamics from the viewpoints of hydrology-oriented silviculture and ecophysiology, all components of evapotranspiration should be measured individually for a minimum of a few of years following thinning. In light of this and similar studies, water resource planners interested in achieving SDG 6 should be cognizant of the effects of forest thinning on the forest water balance because sufficient water supplies are necessary to ensure access to safe, clean water and sanitation by all (Creed and van Noordwijk, 2018; Nath et al., 2020).

5. Conclusions

Based on pre- and post-thinning measurements of sap flux density over a five-year period to estimate the effect of thinning on transpiration from a Japanese cedar stand, the following conclusions have been reached:

1. Due to the thinning, stand-scale transpiration decreased to 71 % of the pre-thinning level in the first year after treatment, and was 100 % and 107 % in the second and third years, respectively, indicating that transpiration recovered to the pre-thinning levels in approximately two to three years.
2. The prompt recovery of transpiration was caused by the large increase in the inner sap flow contribution, rather than the changes in outer sap flux density after thinning.
3. Our conceptual model demonstrates that the higher contribution of inner sap flow (as opposed to outer sap flow) was attributable to the differential ecophysiological responses between upper and lower portions of tree crowns to changing light conditions.

To establish suitable management plans for plantation forests based on hydrology-oriented silviculture, measurements of outer and inner sap flux densities are necessary for at least a few of years after thinning operations. This will ensure the capture of post thinning temporal variabilities in transpiration. Besides quantifying and documenting changes in transpiration, it is recommended that future studies also examine other components of evapotranspiration, namely interception loss and forest floor evaporation, for a few years post treatment. Together, the results of this and future studies would provide a more thorough understanding of alterations to the hydrological cycle by thinning that may be used to advance progress toward achievement of SDG 6.

Funding

Part of this work was supported by JSPS KAKENHI Grant Numbers of JP21H05316 and JP22H02396, and also by the project “Research on adaptation to climate change for forestry and fisheries” from the Agriculture, Forestry and Fisheries Research Council, Japan and the Global Environmental Research Coordination System from Ministry of the Environment of Japan.

CRedit authorship contribution statement

Shin'ichi Iida: Conceptualization, Formal analysis, Investigation, Methodology, Visualization, Writing – original draft, Writing – review & editing. **Shoji Noguchi:** Investigation, Resources, Writing – review & editing. **Delphis F. Levia:** Visualization, Writing – review & editing. **Makoto Araki:** Investigation. **Kyohei Nitta:** Investigation, Resources. **Satoru Wada:** Investigation, Resources. **Yoshito Narita:** Investigation, Resources. **Hiroki Tamura:** Investigation, Resources. **Toshio Abe:** Investigation, Visualization. **Tomonori Kaneko:** Project administration.

Declaration of competing interest

The authors declare that they have no known competing financial interests or personal relationships that could have appeared to influence the work reported in this paper.

Data availability

Data will be made available on request.

Acknowledgements

We appreciate fieldwork assistance provided by the staff of Akita Forestry Research and Training Center.

Appendix A. Supplementary data

Supplementary data to this article can be found online at <https://doi.org/10.1016/j.scitotenv.2023.169060>.

References

- Alkama, R., Cescatti, A., 2016. Biophysical climate impacts of recent changes in global forest cover. *Science* 351, 600–604. <https://doi.org/10.1126/science.aac8083>.
- Bonan, G.B., 2008. Forests and climate change: forcings, feedbacks, and the climate benefits of forests. *Science* 320, 1444–1449. <https://doi.org/10.1126/science.1155121>.
- Bréda, N., Granier, A., Aussenac, G., 1995. Effects of thinning on soil and tree water relations, transpiration and growth in an oak forest (*Quercus petraea* (Matt.) Liebl.). *Tree Physiol.* 15, 295–306. <https://doi.org/10.1093/treephys/15.5.295>.
- del Campo, A.D., González-Sanchis, M., Molina, A.J., Garcia-Prats, A., Ceacero, C.J., Bautista, I., 2019. Effectiveness of water-oriented thinning in two semi-arid forests: the redistribution of increased net rainfall into soil water, drainage and runoff. *For. Ecol. Manag.* 438, 163–175. <https://doi.org/10.1016/j.foreco.2019.02.020>.
- del Campo, A.D., Otsuki, K., Serengil, Y., Blanco, J.A., Yousefpour, R., Wei, X., 2022. A global synthesis on the effects of thinning on hydrological processes: implications for forest management. *For. Ecol. Manag.* 519, 120324 <https://doi.org/10.1016/j.foreco.2022.120324>.
- Cermák, J., Nadezhdina, N., Trcala, M., Simon, J., 2015. Open field-applicable instrumental methods for structural and functional assessment of whole trees and stands. *IForest* 8, 226. <https://doi.org/10.3832/ifer1116-008>.
- Chiu, C.W., Gomi, T., Hiraoka, M., Shiraki, K., Onda, Y., Dung, B.X., 2022. Evaluating changes in catchment-scale evapotranspiration after 50% strip-thinning in a headwater catchment. *Hydrol. Process.* 36, e14611 <https://doi.org/10.1002/hyp.14611>.
- Clearwater, M.J., Meinzer, F.C., Andrade, J.L., Goldstein, G., Holbrook, N.M., 1999. Potential errors in measurement of nonuniform sap flow using heat dissipation probes. *Tree Physiol.* 19, 681–687. <https://doi.org/10.1093/treephys/19.10.681>.
- Creed, I.F., van Noordwijk, M., 2018. Forest and Water on a Changing Planet: Vulnerability, Adaptation and Governance Opportunities. A global assessment report, IUFRO world series, p. 38.

- Dawson, T.E., Mambelli, S., Plamboeck, A.H., Templer, P.H., Tu, K.P., 2002. Stable isotopes in plant ecology. *Annu. Rev. Ecol. Syst.* 33, 507–559. <https://doi.org/10.1146/annurev.ecolsys.33.020602.095451>.
- Delzon, S., Sartore, M., Granier, A., Loustau, D., 2004. Radial profiles of sap flow with increasing tree size in maritime pine. *Tree Physiol.* 24, 1285–1293. <https://doi.org/10.1093/treephys/24.11.1285>.
- Dye, P.J., Olbrich, B.W., Poulter, A.G., 1991. The influence of growth rings in *Pinus patula* on heat pulse velocity and sap flow measurement. *J. Exp. Bot.* 42, 867–870. <https://doi.org/10.1093/jxb/42.7.867>.
- Ellison, D., Morris, C.E., Locatelli, B., Sheil, D., Cohen, J., Murdiyarto, D., Gutierrez, V., van Noordwijk, M., Creed, I.F., Pokorny, J., Gaveau, D., Spracklen, D.V., Tobella, A. B., Ilstedt, U., Teuling, A.J., Gebrehiwot, S.G., Sands, D.C., Muys, B., Verbist, B., Springray, E., Sugandi, Y., Sullivan, G.A., 2017. Trees, forests and water: cool insights for a hot world. *Glob. Environ. Chang.* 43, 51–61. <https://doi.org/10.1016/j.gloenvcha.2017.01.002>.
- Fiora, A., Cescatti, A., 2006. Diurnal and seasonal variability in radial distribution of sap flux density: implications for estimating stand transpiration. *Tree Physiol.* 26, 1217–1225. <https://doi.org/10.1093/treephys/26.9.1217>.
- Forestry Agency, Ministry of Agriculture, Forestry and Fisheries, Japan, 2022. *Annual Report on Trends in Forests and Forestry, Fiscal Year 2021 (in Japanese)*.
- Forrester, D.I., Collopy, J.J., Beadle, C.L., Warren, C.R., Baker, T.G., 2012. Effect of thinning, pruning and nitrogen fertiliser application on transpiration, photosynthesis and water-use efficiency in a young *Eucalyptus nitens* plantation. *For. Ecol. Manag.* 266, 286–300. <https://doi.org/10.1016/j.foreco.2011.11.019>.
- Fuchs, S., Leuschner, C., Link, R., Coners, H., Schuldt, B., 2017. Calibration and comparison of thermal dissipation, heat ratio and heat field deformation sap flow probes for diffuse-porous trees. *Agric. For. Meteorol.* 244, 151–161. <https://doi.org/10.1016/j.agrformet.2017.04.003>.
- Gebauer, R., Volařík, D., Urban, J., Børja, I., Nagy, N.E., Eldhuset, T.D., Krokene, P., 2011. Effect of thinning on anatomical adaptations of Norway spruce needles. *Tree Physiol.* 31, 1103–1113. <https://doi.org/10.1093/treephys/tpq081>.
- Gebauer, R., Volařík, D., Urban, J., Børja, I., Nagy, N.E., Eldhuset, T.D., Krokene, P., 2014. Altered light conditions following thinning affect xylem structure and potential hydraulic conductivity of Norway spruce shoots. *Eur. J. For. Res.* 133, 111–120. <https://doi.org/10.1007/s10342-013-0747-5>.
- Granier, A., 1985. Une nouvelle méthode pour la mesure du flux de sève brute dans le tronc des arbres. *Ann Sci For.* 42, 193–200 [Granier, A., 2007. A New Method of Sap Flow Measurement in Tree Trunks. English Translation by Gash, J.H.C., Granier, A., In: Gash, J.H.C., Shuttleworth, W.J. (eds) *Evaporation, Benchmark Papers in Hydrology 2*. IAHS Press, pp. 61–63].
- Granier, A., Bréda, N., 1996. Modelling canopy conductance and stand transpiration of an oak forest from sap flow measurements. *Ann. Sci. For.* 53, 537–546. <https://doi.org/10.1051/forest:19960233>.
- Guswa, A.J., Tetzlaff, D., Selker, J.S., Carlyle-Moses, D.E., Boyer, E.W., Bruen, M., Cayuela, C., Creed, I.F., van de Giesen, N., Grasso, D., Hannah, D.M., Hudson, J.E., Hudson, S.A., Iida, S., Jackson, R.B., Katul, G.G., Kumagai, T., Llorens, P., Ribeiro, F. L., Michalzik, B., Nanko, K., Oster, C., Pataki, D.E., Peters, C.A., Rinaldo, A., Carretero, D.S., Trifunovic, B., Zalewski, M., Haagsma, M., Levina, D.F., 2020. Advancing ecohydrology in the 21st century: a convergence of opportunities. *Ecohydrology* 13, e2208. <https://doi.org/10.1002/eco.2208>.
- Gyokusen, K., Kobayashi, H., Saito, A., 1994. Seasonal change of light environment and leaf area index in a sugi (*Cryptomeria japonica*) canopy. *J. Jpn. For. Soc.* 76, 465–467. <https://doi.org/10.11519/jjfs1953.76.5.465>.
- Harrington, C.A., Reukema, D.L., 1983. Initial shock and long-term stand development following thinning in a Douglas-fir plantation. *For. Sci.* 29, 33–46. <https://doi.org/10.1093/forestscience/29.1.33>.
- Iida, S., Kobayashi, Y., Tanaka, T., 2003. Continuous and long-term measurement of sap flux using Granier method. *J. Jpn. Soc. Hydrol. Water Resour.* 16, 13–22. [https://doi.org/10.3178/jjshwr.16.13 \(in Japanese with English abstract\)](https://doi.org/10.3178/jjshwr.16.13 (in Japanese with English abstract)).
- Iida, S., Noguchi, S., Shimizu, T., Kaneko, T., 2017. Relationships of sapwood area and width of bark to diameter at breast height of Japanese cedar planted in the Tohoku district, Japan. *J. Jpn. Assoc. Hydrol. Sci.* 47, 3–9. [https://doi.org/10.4145/jahs.47.3 \(in Japanese with English abstract\)](https://doi.org/10.4145/jahs.47.3 (in Japanese with English abstract)).
- Iida, S., Takeuchi, S., Araki, M., Shimizu, T., Noguchi, S., Sawano, S., Kaneko, T., 2018. Duration of available sap flux density data measured by sensors applied to Japanese cedar. *J. Jpn. Soc. Hydrol. Water Resour.* 31, 280–291. [https://doi.org/10.3178/jjshwr.31.280 \(in Japanese with English abstract\)](https://doi.org/10.3178/jjshwr.31.280 (in Japanese with English abstract)).
- Iida, S., Shimizu, T., Tamai, K., Kabeya, N., Shimizu, A., Ito, E., Ohnuki, Y., Chann, S., Levina, D.F., 2020a. Evapotranspiration from the understory of a tropical dry deciduous forest in Cambodia. *Agric. For. Meteorol.* 295, 108170. <https://doi.org/10.1016/j.agrformet.2020.108170>.
- Iida, S., Shimizu, T., Shinohara, Y., Takeuchi, S., Kumagai, T., 2020b. The necessity of sensor calibration for the precise measurement of water fluxes in forest ecosystems. In: Levina, D.F., Carlyle-Moses, D.E., Iida, S., Michalzik, B., Nanko, K., Tischer, A. (Eds.), *Forest-Water Interactions*. Ecological Studies Series, No.240. Springer, pp. 29–54. https://doi.org/10.1007/978-3-030-26086-6_2.
- Iida, S., Takeuchi, S., Shinozaki, K., Araki, M., 2022. Calibration of sap flow techniques using the root-ball weighing method in Japanese cedar trees. *Trees* 36, 1747–1759. <https://doi.org/10.1007/s00468-022-02325-w>.
- Jiménez, E., Vega, J.A., Pérez-Gorostiaga, P., Cuñías, P., Fonturbel, T., Fernández, C., Madrigal, J., Hernandez, C., Guizarro, M., 2008. Effects of pre-commercial thinning on transpiration in young post-fire maritime pine stands. *Forestry* 81, 543–557. <https://doi.org/10.1093/forestry/cpn032>.
- Jones, J.A., Wei, X., Archer, E., Bishop, K., Blanco, J.A., Ellison, D., Gush, M.B., McNulty, S.G., van Noordwijk, M., Creed, I.F., 2020. Forest-water interactions under global change. In: Levina, D.F., Carlyle-Moses, D.E., Iida, S., Michalzik, B., Nanko, K., Tischer, A. (Eds.), *Forest-Water Interactions*. Ecological Studies Series, No.240. Springer, pp. 589–624. https://doi.org/10.1007/978-3-030-26086-6_24.
- Kaneko, T., Takeda, K., Noguchi, S., Oohara, H., Fujieda, M., 2010. Comparison of runoff characteristics among three close catchments of artificial Sugi (*Cryptomeria japonica*) forest in a snowy region. *J. Jpn. For. Soc.* 92, 208–216. [https://doi.org/10.4005/jjfs.92.208 \(in Japanese with English abstract\)](https://doi.org/10.4005/jjfs.92.208 (in Japanese with English abstract)).
- Komatsu, H., 2007. Relationship between stem density and interception ratio for coniferous plantation forests in Japan. *J. Jpn. For. Soc.* 89, 217–220. [https://doi.org/10.4005/jjfs.89.217 \(in Japanese with English abstract\)](https://doi.org/10.4005/jjfs.89.217 (in Japanese with English abstract)).
- Komatsu, H., 2020. Modeling evapotranspiration changes with managing Japanese cedar and cypress plantations. *For. Ecol. Manag.* 475, 118395. <https://doi.org/10.1016/j.foreco.2020.118395>.
- Komatsu, H., Shinohara, Y., Kume, T., Otsuki, K., 2008. Relationship between annual rainfall and interception ratio for forests across Japan. *For. Ecol. Manag.* 256, 1189–1197. <https://doi.org/10.1016/j.foreco.2008.06.036>.
- Komatsu, H., Shinohara, Y., Nogata, M., Tsuruta, K., Otsuki, K., 2013. Changes in canopy transpiration due to thinning of a *Cryptomeria japonica* plantation. *Hydrol. Res. Lett.* 7, 60–65. <https://doi.org/10.3178/hrl.7.60>.
- Kosugi, Y., Katsuyama, M., 2007. Evapotranspiration over a Japanese cypress forest. II. Comparison of the eddy covariance and water budget methods. *J. Hydrol.* 334, 305–311. <https://doi.org/10.1016/j.jhydrol.2006.05.025>.
- Kubota, T., Tsuboyama, Y., Nobuhiro, T., 2018. Effects of thinning on canopy interception loss, evapotranspiration, and runoff in a small headwater *Chamaecyparis obtusa* catchment in Hitachi Ohta Experimental Watershed in Japan. *Bull. For. For. Prod. Res. Inst.* 17, 63–73. <https://doi.org/10.20756/ffpri.17.1.63>.
- Kumagai, T., Aoki, S., Shimizu, T., Otsuki, K., 2007. Sap flow estimates of stand transpiration at two slope positions in a Japanese cedar forest watershed. *Tree Physiol.* 27, 161–168. <https://doi.org/10.1093/treephys/27.2.161>.
- Kumagai, T., Tateishi, M., Shimizu, T., Otsuki, K., 2008. Transpiration and canopy conductance at two slope positions in a Japanese cedar forest watershed. *Agric. For. Meteorol.* 148, 1444–1455. <https://doi.org/10.1002/hyp.7338>.
- Lagergren, F., Lankreijer, H., Kučera, J., Cienciala, E., Mölder, M., Lindroth, A., 2008. Thinning effects on pine-spruce forest transpiration in central Sweden. *For. Ecol. Manag.* 255, 2312–2323. <https://doi.org/10.1016/j.foreco.2007.12.047>.
- Leite-Filho, A.T., Soares-Filho, B.S., Davis, J.L., Abrahão, G.M., Börner, J., 2021. Deforestation reduces rainfall and agricultural revenues in the Brazilian Amazon. *Nat. Commun.* 12, 2591. <https://doi.org/10.1038/s41467-021-22840-7>.
- Levia, D.F., Creed, I.F., Hannah, D.M., Nanko, K., Boyer, E.W., Carlyle-Moses, D.E., van de Giesen, N., Grasso, D., Guswa, A.J., Hudson, J.E., Hudson, S.A., Iida, S., Jackson, R.B., Katul, G.G., Kumagai, T., Llorens, P., Ribeiro, F.L., Pataki, D.E., Peters, C.A., Carretero, D.S., Selker, J.S., Tetzlaff, D., Zalewski, M., Bruen, M., 2020. Homogenization of the terrestrial water cycle. *Nat. Geosci.* 13, 656–658. <https://doi.org/10.1038/s41561-020-0641-y>.
- Mäkinen, H., Isomäki, A., 2004. Thinning intensity and growth of Scots pine stands in Finland. *For. Ecol. Manag.* 201, 311–325. <https://doi.org/10.1016/j.foreco.2004.07.016>.
- Medhurst, J.L., Battaglia, M., Beadle, C.L., 2002. Measured and predicted changes in tree and stand water use following high-intensity thinning of an 8-year-old *Eucalyptus nitens* plantation. *Tree Physiol.* 22, 775–784. <https://doi.org/10.1093/treephys/22.11.775>.
- Mohamed, G.H., Parker, W.C., 1999. Photosynthetic acclimation in eastern hemlock [*Tsuga canadensis* (L.) Carr.] seedlings following transfer of shade-grown seedlings to high light. *Trees* 13, 117–124. <https://doi.org/10.1007/PL00009743>.
- Molina, A.J., del Campo, A.D., 2012. The effects of experimental thinning on throughfall and stemflow: a contribution towards hydrology-oriented silviculture in Aleppo pine plantations. *For. Ecol. Manag.* 269, 206–213. <https://doi.org/10.1016/j.foreco.2011.12.037>.
- Monteith, J.L., Unsworth, M.H., 1990. *Principles of Environmental Physics*, 2nd edition. Edward Arnold.
- Morikawa, Y., Hattori, S., Kiyono, Y., 1986. Transpiration of a 31-year-old *Chamaecyparis obtusa* Endl. stand before and after thinning. *Tree Physiol.* 2, 105–114. <https://doi.org/10.1093/treephys/2.1-2.3.105>.
- Nadezhkina, N., Vandegehuchte, M.W., Steppe, K., 2012. Sap flux density measurements based on the heat field deformation method. *Trees* 26, 1439–1448. <https://doi.org/10.1007/s00468-012-0718-3>.
- Nath, T.K., Jashimuddin, M., Inoue, M., 2020. Achieving sustainable development goals through participatory forest management: examples from South-Eastern Bangladesh. *Nat. Resour. Forum.* 44, 353–368. <https://doi.org/10.1111/1477-8947.12209>.
- Noguchi, S., Kaneko, T., Oohara, H., Tamura, H., Hirai, K., 2010. Meteorological characteristics in Nagasaka Experimental Watershed, Akita, Japan. *Bull For For Prod Res Inst.* 9, 167–191.
- Ohmasa, Y., Noguchi, S., Okada, Y., Iida, S., 2018. Forest maintenance projects for sustainable use of forest resources in Japan. *J. Jpn. Soc. Hydrol. Water Resour.* 31, 414–427. [https://doi.org/10.3178/jjshwr.31.414 \(in Japanese with English abstract\)](https://doi.org/10.3178/jjshwr.31.414 (in Japanese with English abstract)).
- Onda, Y., Gomi, T. (Eds.), 2021. *Forest Management Strategies That Maximize Water Resources: A Proposal Based on Large-scale Monitoring Data*. The University of Tokyo Press (in Japanese).
- Oren, R., Sperry, J.S., Katul, G.G., Pataki, D.E., Ewers, B.E., Phillips, N., Schäfer, K.V.R., 1999. Survey and synthesis of intra- and interspecific variation in stomatal sensitivity to vapour pressure deficit. *Plant Cell Environ.* 22, 1515–1526. <https://doi.org/10.1046/j.1365-3040.1999.00513.x>.
- Park, J., Kim, T., Moon, M., Cho, S., Ryu, D., Kim, H.S., 2018. Effects of thinning intensities on tree water use, growth, and resultant water use efficiency of 50-year-old *Pinus koraiensis* forest over four years. *For. Ecol. Manag.* 408, 121–128. <https://doi.org/10.1016/j.foreco.2017.09.031>.

- Pearcy, R.W., Sims, D.A., 1994. Photosynthetic acclimation to changing light environments: scaling from the leaf to the whole plant. In: Caldwell, M.M., Pearcy, R. W. (Eds.), *Exploitation of Environmental Heterogeneity by Plants*. Academic Press, pp. 145–174.
- Phillips, N., Oren, R.A., 1998. Comparison of daily representations of canopy conductance based on two conditional time-averaging methods and the dependence of daily conductance on environmental factors. *Ann. Sci. For.* 55, 217–235. <https://doi.org/10.1051/forest:19980113>.
- R Core Team, 2023. *R: A Language and Environment for Statistical Computing*. R Foundation for Statistical Computing, Vienna (Austria).
- Richardson, S.J., Hurst, J.M., Easdale, T.A., Wisser, S.K., Griffiths, A.D., Allen, R.B., 2011. Diameter growth rates of beech (*Nothofagus*) trees around New Zealand. *N. Z. J. For.* 56, 3–11.
- Shimizu, T., Kumagai, T., Kobayashi, M., Tamai, K., Iida, S., Kabeya, N., Ikawa, R., Tateishi, M., Miyazawa, Y., Shimizu, A., 2015. Estimation of annual forest evapotranspiration from a coniferous plantation watershed in Japan (2): comparison of eddy covariance, water budget and sap-flow plus interception loss. *J. Hydrol.* 522, 250–264. <https://doi.org/10.1016/j.jhydrol.2014.12.021>.
- Shinohara, Y., Tsuruta, K., Ogura, A., Noto, F., Komatsu, H., Otsuki, K., Maruyama, T., 2013. Azimuthal and radial variations in sap flux density and effects on stand-scale transpiration estimates in a Japanese cedar forest. *Tree Physiol.* 33, 550–558. <https://doi.org/10.1093/treephys/tpt029>.
- Shinohara, Y., Iida, S., Oda, T., Katayama, A., Tsuruta, K., Sato, T., Tanaka, N., Su, M.-P., Laplace, S., Kijidani, Y., Kume, T., 2022. Are calibrations of sap flow measurements based on thermal dissipation needed for each sample in Japanese cedar and cypress trees? *Trees* 36, 1219–1229. <https://doi.org/10.1007/s00468-022-02283-3>.
- Skubel, R.A., Khomik, M., Brodeur, J.J., Thorne, R., Arain, M.A., 2017. Short-term selective thinning effects on hydraulic functionality of a temperate pine forest in eastern Canada. *Ecohydrology* 10, e1780. <https://doi.org/10.1002/eco.1780>.
- Smith, C., Baker, J.C.A., Spracklen, D.V., 2023. Tropical deforestation causes large reductions in observed precipitation. *Nature* 615, 270–275. <https://doi.org/10.1038/s41586-022-05690-1>.
- Spracklen, D.V., Garcia-Carreras, L.J.G.R.L., 2015. The impact of Amazonian deforestation on Amazon basin rainfall. *Geophys. Res. Lett.* 42, 9546–9552. <https://doi.org/10.1002/2015GL066063>.
- Steppe, K., De Pauw, D.J., Doody, T.M., Teskey, R.O., 2010. A comparison of sap flux density using thermal dissipation, heat pulse velocity and heat field deformation methods. *Agric. For. Meteorol.* 150, 1046–1056. <https://doi.org/10.1016/j.agrformet.2010.04.004>.
- Sun, X., Onda, Y., Otsuki, K., Kato, H., Hirata, A., Gomi, T., 2014. The effect of strip thinning on tree transpiration in a Japanese cypress (*Chamaecyparis obtusa* Endl.) plantation. *Agric. For. Meteorol.* 197, 123–135. <https://doi.org/10.1016/j.agrformet.2014.06.011>.
- Sun, X., Onda, Y., Otsuki, K., Kato, H., Gomi, T., Liu, X., 2017. Change in evapotranspiration partitioning after thinning in a Japanese cypress plantation. *Trees* 31, 1411–1421. <https://doi.org/10.1007/s00468-017-1555-1>.
- Takeuchi, S., Shinozaki, K., Matsushima, D., Iida, S., 2020. Calibration of the heat ratio method by direct measurements of transpiration with the weighing root-ball method for *Michelia figo*. *Acta Hort.* 1300, 21–28. <https://doi.org/10.17660/ActaHortic.2020.1300.4>.
- Tateishi, M., Xiang, Y., Saito, T., Otsuki, K., Kasahara, T., 2015. Changes in canopy transpiration of Japanese cypress and Japanese cedar plantations because of selective thinning. *Hydrol. Process.* 29, 5088–5097. <https://doi.org/10.1002/hyp.10700>.
- Tie, Q., Hu, H., Tian, F., Holbrook, N.M., 2018. Comparing different methods for determining forest evapotranspiration and its components at multiple temporal scales. *Sci. Total Environ.* 633, 12–29. <https://doi.org/10.1016/j.scitotenv.2018.03.082>.
- Wang, Y., Wei, X., del Campo, A.D., Winkler, R., Wu, J., Li, Q., Liu, W., 2019. Juvenile thinning can effectively mitigate the effects of drought on tree growth and water consumption in a young *Pinus contorta* stand in the interior of British Columbia, Canada. *For. Ecol. Manag.* 454, 117667. <https://doi.org/10.1016/j.foreco.2019.117667>.
- Wilson, K.B., Hanson, P.J., Mulholland, P.J., Baldocchi, D.D., Wullschleger, S.D., 2001. A comparison of methods for determining forest evapotranspiration and its components: sap-flow, soil water budget, eddy covariance and catchment water balance. *Agric. For. Meteorol.* 106, 153–168. [https://doi.org/10.1016/S0168-1923\(00\)00199-4](https://doi.org/10.1016/S0168-1923(00)00199-4).
- Yamanaka, T., 2018. Root functional change achieves water source separation under vegetation succession. *Ecohydrology* 11, e1985. <https://doi.org/10.1002/eco.1985>.